Bathymetry Retrieval from Hyperspectral Remote Sensing Data in Optical-Shallow Water

Sheng Ma, Zui Tao, Xiaofeng Yang, *Member, IEEE*, Yang Yu, Xuan Zhou, and Ziwei Li

***Abstract*— In this paper, an algorithm for estimating shallow-water depth from hyperspectral data is proposed. This methodology is based on the different responses of shallow-water reflectance on depth and substrate type. Two parameters—similarity coefficient and Pearson correlation coefficient—are introduced to describe the different types of responses, and a linear logarithm ratio model is established. Using Hyperion data over the coastal regions of O'Ahu Island and Saint Thomas Island, the retrieved bathymetry is compared with the airborne LIDAR data. The validation results show that the proposed method has good performance, and the root mean square error is less than 1.5 m over shallow water (shallower than 20 m).**

***Index Terms*— Bathymetry, Hyperion, hyperspectral, LIDAR, remote sensing.**

I. Introduction

BATHYMETRIC measurement of shallow water is of fundamental importance to coastal benthic environment research and resource management. The conventional bathymetric survey approach is to use ship-sounding techniques, which can provide high-precision data but is costly and inefficient [1]. With the development of optical remote sensing techniques, these techniques can provide quantitative information on shallow water and benthic habitats quickly and at low cost [2]. The potential to apply optical remote sensing to derive shallow-water depths has been discussed for more than three decades, and several case studies have demonstrated its utility [3]–[8].

Since the first use of aerial photography over clear shallow water, many practical algorithms have been proposed. Most of these algorithms are applied to high-resolution multispectral data, such as Landsat/TM [9], POT/HRV [10], or IKNOS [11]. These algorithms can be categorized into two groups: empirical approaches and semi-analytical models. Based on the fundamental principle that the radiation attenuation varies with wavelength as it penetrates the water column, many empirical methods have been constructed [1], [3], [5], [9], [12], [13]. Because too many coefficients in these methods need to be calibrated individually for different water conditions, they are not easily implemented in different areas, and the accuracy of estimated depth is influenced by complex benthic types [7]. To solve this problem, Stumpf *et al*. [4] developed a semi-analytical model that established a linear relationship between the ratio of water depth and the reflectance of green and blue bands. Although this method has only two parameters and is more robust, these parameters also need to be calibrated with field data for different water areas. Many studies have also noted that shallow-water bathymetry is difficult to derive accurately over high-albedo substrates with the ratio of green and blue bands [14]–[16].

The booming developments of hyperspectral remote sensing techniques, especially the great improvements in the signal-to-noise ratio (SNR) of hyperspectral data, have caught researchers' attention and their interest in applying hyperspectral techniques to bathymetric mapping. A neural network method was used by Sandidge and Holyer to derive bathymetry from Airborne Visible/Infrared Imaging Spectrometer (AVIRIS) imagery of Florida water [17]. To extract the optical water properties, bottom reflectance and water depth simultaneously, Lee *et al*. [18] presented a semi-analytical model that can be applied to Hyperion [19], [20], and AVIRIS [7] data. An algorithm similar to Lee's with simpler assumptions was proposed by Adler-Golden *et al.* [21]. Several studies have used or extended Lee's model to clear waters [22]–[25], and a spectrum-matching and look-up-table methodology has been developed and proven applicable to retrieve water depth [26]. All these successful study cases have indicated the advantages of hyperspectral data in clear shallow-water bathymetric estimation.

In this paper, a new method that can estimate clear shallow-water depth (0–30 m) from hyperspectral data is proposed. The basis of the method is the different spectral responses on changes of benthic and water depth. Two parameters were introduced in the model to describe the different responses. Using the Hyperion data collected over the coastal regions of O'Ahu Island and Saint Thomas Island as examples, the ability of this method to estimate bathymetry is presented. The result is compared with airborne LIDAR bathymetry data to assess the accuracy. The theory of the method is discussed in Section II, and a description of the data processing is given in

Manuscript received September 3, 2012; revised December 27, 2012; accepted February 15, 2013. Date of publication March 28, 2013; date of current version December 12, 2013. This work was supported by Chinese Public Science and Technology Research Funds Projects of Ocean under Grant 201005009 and Grant 201005011. *(Corresponding author: X. Yang.)*

The authors are with the State Key Laboratory of Remote Sensing Science, Jointly Sponsored by the Institute of Remote Sensing Applications of Chinese Academy of Sciences and Beijing Normal University, Beijing 100101, China (e-mail: masheng1987@ gmail.com; taozui8421@163.com; yangxf@irsa.ac.cn; yuyang@irsa.ac.cn; youme_zx@163.com; lizw@irsa.ac.cn).

Color versions of one or more of the figures in this paper are available online at http://ieeexplore.ieee.org.

Digital Object Identifier 10.1109/TGRS.2013.2248372

Section III. Detailed information of the experimental results and validation is described in Section IV. A discussion and conclusion is given in Section V.

II. Methodology

According to Beer's Law, light decreases exponentially in water as the depth increases [5]. On the basis of this principle, Lyzenga (1978) showed that the observed reflectance R_w could be expressed by depth and bottom albedo as

$$R_W = (A_d - R_\infty)\exp(-gz) + R_\infty \tag{1}$$

where R_∞ is the water column reflectance if the water were optically deep, A_d is the bottom albedo, z is the depth, and g is a function of the diffuse attenuation coefficients for both downwelling and upwelling light [4]. This relationship shows that the changes of observed reflectance mainly come from the variation of depth and bottom albedo, while the water's optical properties are assumed to be uniform. As reflected in the spectrum, whether the depth or benthic type changes, the spectrum from 480 to 610 nm varies obviously [15].

According to Holden *et al.* [27]–[29], the response types of spectral curves (from 480 to 610 nm) on bottom type and water depth are different. When the water depth is fixed and the bottom type varies, the shape of the spectrum will change. If the bottom status stays the same and the water depth varies, the values of the spectrum will change but the shape will have little difference. If the response types can be distinguished and the influence of bottom albedo on the observed spectrum is removed, the remaining changes will all be caused by water-depth variation.

Among the processing technologies of hyperspectral data, the Pearson correlation coefficient (CC) and similarity coefficient (SC) have been used to describe the matching degrees of spectrum curves. However, the former has the advantage of using correlation functions to detect similarities in spectral shapes [30]. The SC is the cosine form of the spectral angle and is used as a measurement of the difference between two spectrum vectors. Using the two parameters to depict the changes of spectral shapes and the gross variation of the spectrum vector, a method to derive bathymetry data is established as follows.

1) The spectrum of reflectance over the water area where the depth is close to 0 m is taken as a reference spectrum (0–0.15 m). The reference spectrum R_0 is derived by averaging the spectrum data of these pixels, which are located by *in situ* bathymetry data. The spectrum of other similar water areas, where the water depth is close to zero, can also be used as a reference spectrum.
2) After obtaining the reference spectrum, the CC and SC of pixel i can be defined as follows:

$$\mathrm{CC}(i) = \frac{\sum_{j=1}^{N}(R_{i,j} - \overline{R_i})(R_{0,j} - \overline{R_0})}{\sqrt{\sum_{j=1}^{N}(R_{i,j} - \overline{R_i})^2 * \sum_{j=1}^{N}(R_{0,j} - \overline{R_0})^2}} + 1 \tag{2}$$

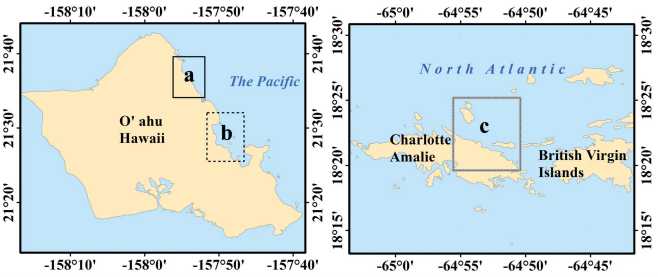

Fig. 1. Locations of Hyperion data used in this paper. The solid, dashed, and gray boxes represent the three Hyperion data imaged areas.

$$\mathrm{SC}(i) = \frac{\sum_{j=1}^{N} R_{i,j} * R_{0,j}}{\sqrt{\sum_{j=1}^{N} R_{i,j}^2}\sqrt{\sum_{j=1}^{N} R_{0,j}^2}} + 1. \tag{3}$$

In (2) and (3), N is the number of all bands between 480 and 610 nm. $R_{i,j}$ is the spectral reflectance of band j of pixel i, $R_{0,j}$ is the reference spectral reflectance of band j, and $\overline{R_i}$($\overline{R_0}$) is the average of all bands of $R_{i,j}$($R_{0,j}$). In these two formulas, a constant is added to ensure that the values are always positive.

3) Referring to the Stumpf *et al.* model and the natural logarithmic relationship between water depth z and observed reflectance R_w, the water depth z of pixel i is estimated by the natural logarithmic ratio between SC and CC as follows:

$$z(i) = k_1 \frac{\ln(n\mathrm{SC}(i))}{\ln(n\mathrm{CC}(i)} - k_0 \tag{4}$$

where k_1 is a tunable constant to scale the ratio to depth, n is a fixed constant that ensures the natural logarithms remain positive for every condition, and k_0 is the offset. In the expression, the influence of bottom type is removed via the ratio between SC and CC.

III. Data Processing

A. Hyperspectral Remote Sensing Data Preparation

In this paper, three Hyperion data over the coast of O'Ahu, Hawaii, and Saint Thomas Island (Fig. 1) were applied to demonstrate the proposed algorithm. Hyperion is a hyperspectral sensor on board NASAs EO-1 platform that can provide hyperspectral imagery with 220 spectral bands (from 430 to 2400 nm) with a 30-m resolution (for nadir viewing) [31]. Although the SNR of the Hyperion data is not as good as SeaWiFS or MODIS, its spectral and spatial characteristics are significantly better. Therefore, these data are more suited to the coastal water and coral reef environment research [19]. The three Hyperion images used here are the L1GST data downloaded from the U.S. Geological Survey (USGS) website. The RGB true-color composition images are shown in Fig. 2, from which we can determine that the benthic habitat of these areas is complex.

To use our method on these data, many preprocessing steps are required. First, these images were subset to 155 bands from 430 to 2400 nm by removing corrupted bands,

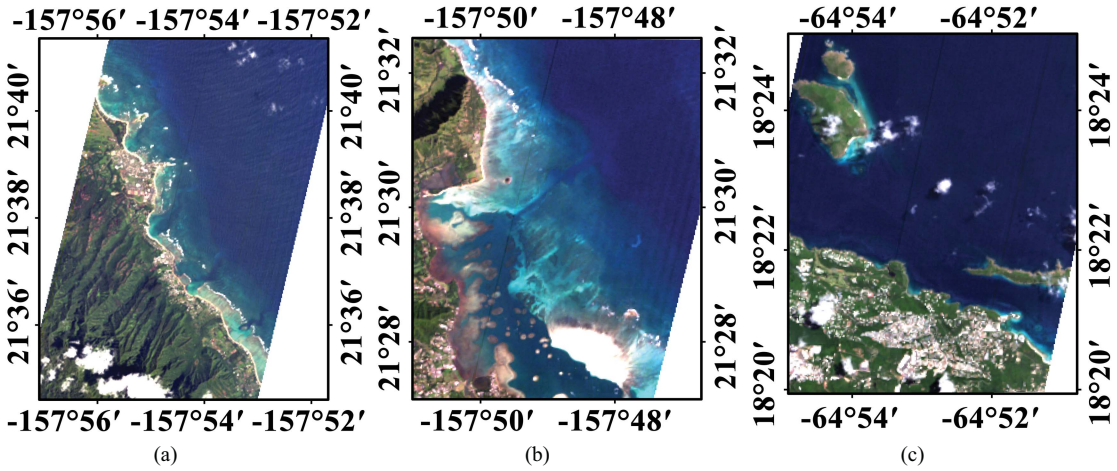

Fig. 2. RGB true-color composition images of the Hyperion data used in this paper. The RGB composition bands are the following. Red: band 22. Green: band 12. Blue: band 4. The pixel resolution of these data are 30 m (a) obtained at 20:45:43 GMT, March 13th, 2011. (b) Obtained at 20:52:36 GMT, February 6th, 2010. (c) Obtained at 14:22:52 GMT, June 24th, 2007.

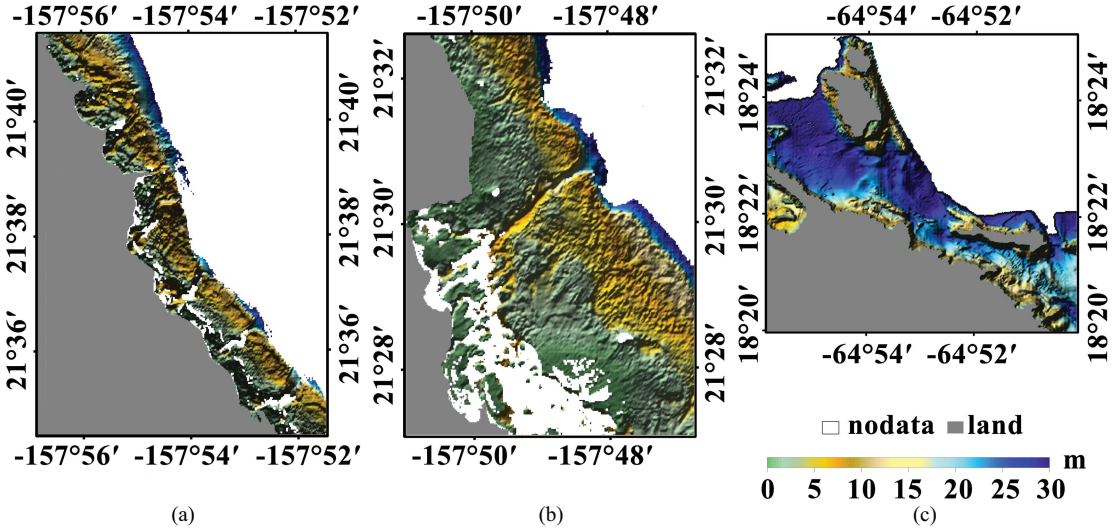

Fig. 3. Airborne LIDAR bathymetry data used in this paper. Data (a) and (b) were collected in 2000 at a resolution of approximately 4 m, and (c) was collected in 2011 at a resolution of approximately 3 m. The vertical accuracy of the data is better than ±15 cm (1 sigma), and the horizontal accuracy is ±3 m.

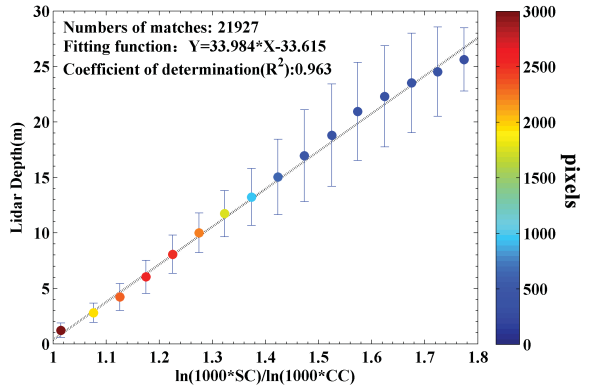

Fig. 4. Scatter plots of the ratio of the natural logarithm for SC and CC versus LIDAR data shown in Fig. 3(a).

and they were converted to absolute radiance images using the calibration parameters. Then, the modified normalized difference water index (MNDWI) [32] was applied to extract the water region, and a MODTRAN-4-based atmospheric correction algorithm [33] was used on each pixel to create reflectance images. Then, sun glint correction was applied to these data following the method presented by Tiit Kutser [34]. After applying the above process, the images can be used to perform our water depth retrieval method.

B. Bathymetry Data Preparation

The *in situ* bathymetry data used in this research were collected by the airborne LIDAR. The locations of these data are shown in Fig. 1, and the bathymetry data are shown in Fig. 3. The data shown in Fig. 3(a) and (b) were collected in the year 2000 using the Scanning Hydrographic Operational Airborne Lidar Survey (SHOALS) instrument. The surveys were compiled by the U.S. Naval Oceanographic Office, U.S. Geological Service, and U.S. Army Corps of Engineers, Honolulu District. The average distance between the irregularly spaced, nongridded SHOALS data points was 4 m. We used

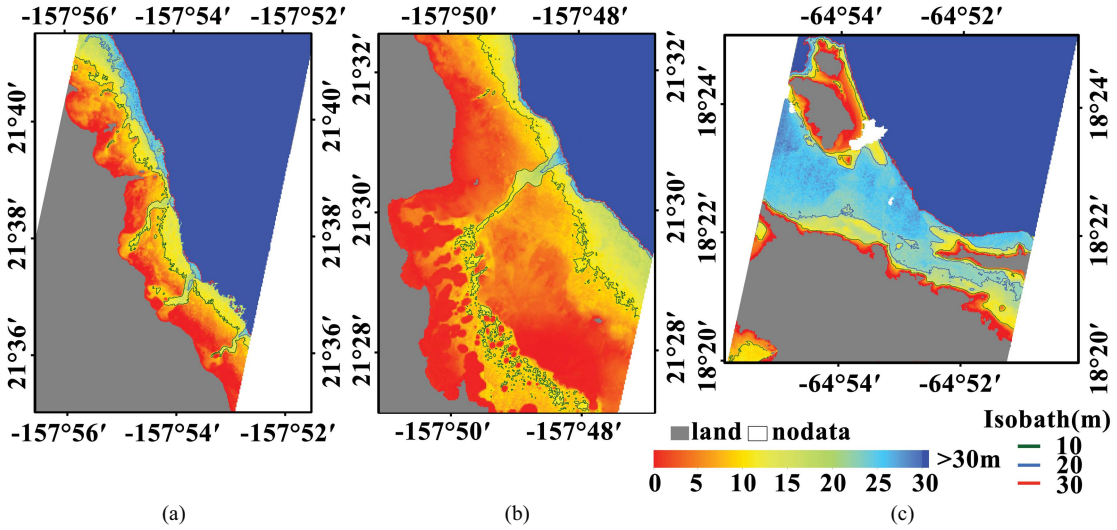

Fig. 5. Water depth distribution maps derived from the Hyperion data using the model proposed in the paper. The lines in these maps are isobaths with 10-m intervals. (a)–(c) are derived from data shown in Fig. 2(a)–(c) respectively.

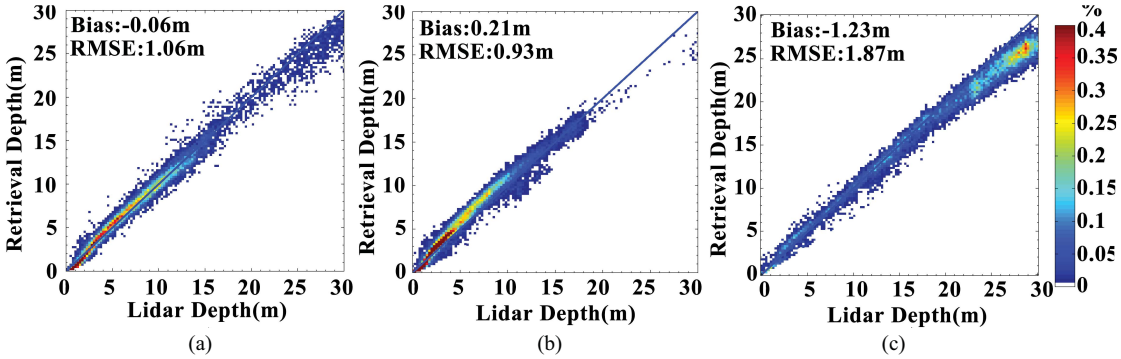

Fig. 6. Comparison of the retrieved depths of the region (shown in Fig. 5) versus the LIDAR depths (shown in Fig. 3). (a)–(c) was derived by comparison with model retrieved result shown in Fig. 5(a)–(c) and field data shown in Fig. 3(a)–(c), respectively. The density color scale represents the percentage of total data within a 0.25 m bin size.

a continuous curvature surface gridding algorithm to rasterize these SHOALS–LIDAR data. The data shown in Fig. 3(c) were collected in the year 2011 using Fugro Airborne LIDAR. The surveys were compiled for NOAAs NOS/NCCOS/CCMA Biogeography Branch, the University of New Hampshire and the National Park Service. The data were gridded into 3 × 3 m. All these bathymetry data had been corrected to depths referenced to mean lower low water (MLLW) heights. The data were resampled to a resolution of 30 m and were co-registered with the Hyperion data to compare them conveniently [2].

IV. Results and Validation

A. Bathymetry Retrieval

To fit the coefficients in (4), the Hyperion data shown in Fig. 2(a) and the bathymetric data shown in Fig. 3(a) were used. First, pixels where the depth was less than 0.15 m were located according to the bathymetric data. Then, the reflectance of every band of these pixels was averaged to derive the reference spectrum from 480 to 610 nm (for Hyperion, the number of bands ranges from 7 to 19). Following (2) and (3), the SC and CC values were calculated pixel by pixel. The parameter n in (4) was taken as 1000 to ensure that the logarithms of SC and CC would always be positive. In the

TABLE I
Error Distribution of Estimated Depths Versus LIDAR Depths With 5-m Intervals

Hyperion Data	Water Depth (m)	Bias (m)	RMSE (m)	Numbers
O'Ahu Island(a)	0–5	0.02	0.58	8090
	5–10	0.27	0.72	6250
	10–15	−0.01	1.05	4282
	15–20	−0.02	1.46	1184
	20–25	−0.81	1.87	858
	25–30	−1.95	2.57	1263
O'Ahu Island(b)	0–5	0.22	0.62	23662
	5–10	0.89	1.18	10388
	10–15	0.18	1.26	4255
	15–20	−0.16	0.99	1613
	20–25	−1.13	1.73	257
	25–30	−2.95	3.35	312
Saint Thomas Island	0–5	0.30	0.76	2048
	5–10	-0.03	0.99	1703
	10–15	−0.27	0.97	2697
	15–20	−0.39	1.00	2725
	20–25	−1.43	1.74	4454
	25–30	−2.41	2.62	7809

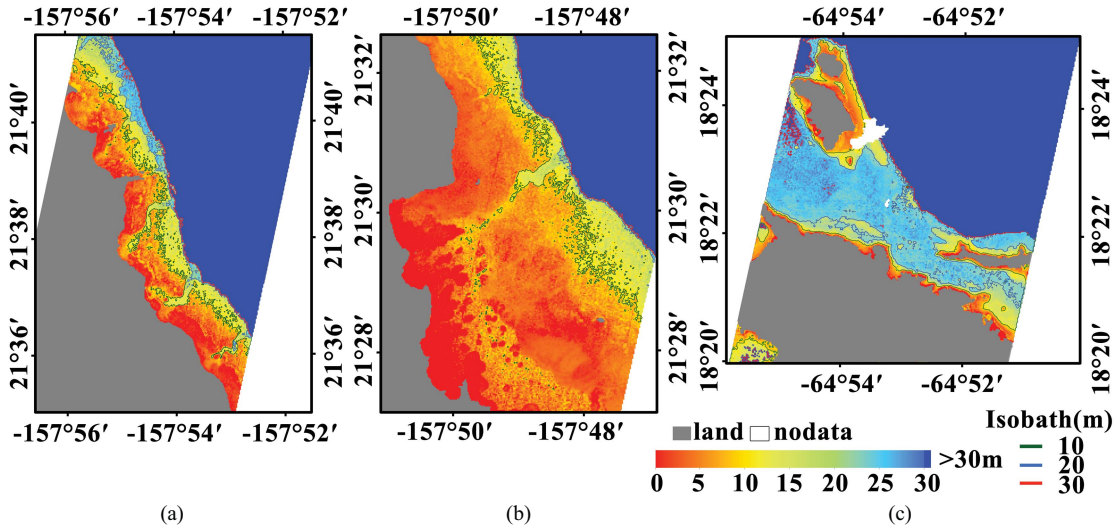

Fig. 7. Water depth distribution maps derived from the Hyperion data using Stumpf's linear transform method. The lines in these maps are isobaths with 10-m intervals. (a)–(c) are derived from data shown in Fig. 2(a)–(c) respectively.

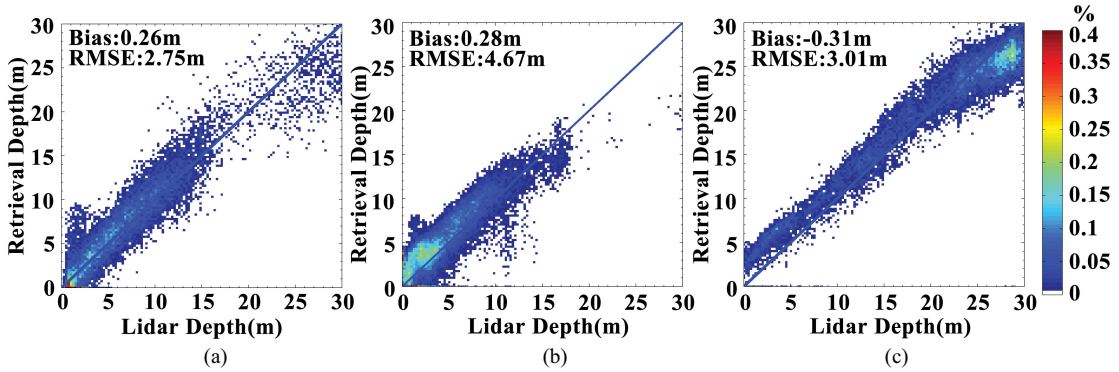

Fig. 8. Comparison of the retrieved depths using Stumpf's method versus the LIDAR depths (shown in Fig. 3). (a)–(c) was derived by comparison with Stumpf's model retrieved result shown in Fig. 7(a)–(c) and field data shown in Fig. 3(a)–(c), respectively. The density color scale represents the percentage of total data within a 0.25 m bin size.

end, using the logarithm ratio of SC and CC and the LIDAR depth, the coefficients in (4) were calculated. The scatter plots and the function are shown in Fig. 4. The high correlation coefficient (0.987) and coefficient of determination (0.963) indicated an almost perfect linear relationship. According to the above processing, we obtained the new model as follows:

$$z(i) = 33.984 * \frac{\ln(1000\mathrm{SC}(i))}{\ln(1000\mathrm{CC}(i))} - 33.615. \qquad (5)$$

Taking the reference spectrum from the Hyperion data shown in Fig. 2(a), the estimated bathymetry data were obtained using (5). To maintain unity with the LIDAR data, −0.17, −0.14, and −0.31 m corrections were applied to correct for tides (the tide data came from NOAAs Tide Predictions and XTide Tide Prediction Server websites). The retrieval bathymetry results are shown in Fig. 5. The lines in these maps are isobaths with 10-m intervals.

B. Validation

The estimated depths versus the LIDAR depths were plotted for the data in Fig. 6. The plots were generated by binning the estimated depths by the LIDAR depths. After removing land and cloud pixels, 21 927, 40 487, and 21 436 matched pixels were left for the three cases. The root mean square errors (RMSEs) of estimated depths versus LIDAR depths are 0.84, 0.93, and 1.87 m for the three images. The figure shows that the new method is well behaved over these three water areas. However, the accuracy of the third is not as good as the first two. To find the reason for this result and to analyze the stability of the method over different water depths, the bias and RMSEs with intervals of 5 m of depth from 0 to 30 m were calculated and are shown in Table I. The table shows that the retrieval results of the three study areas have consistent accuracy for shallow water ($<= 20$ m) but underestimated the depth over deep water (> 20 m). Compared with the data shown in Fig. 6(a) and (b), a much greater water depth appears in Fig. 6(c), which reduced the overall accuracy. From the table, the accuracies over the three areas are close to each other when the depth is shallower than 20 m.

To further analyze the applicability of the proposed method, the linear transform method presented by Stumpf *et al.* was applied to the same data (Figs. 7 and 8). One-tenth of the

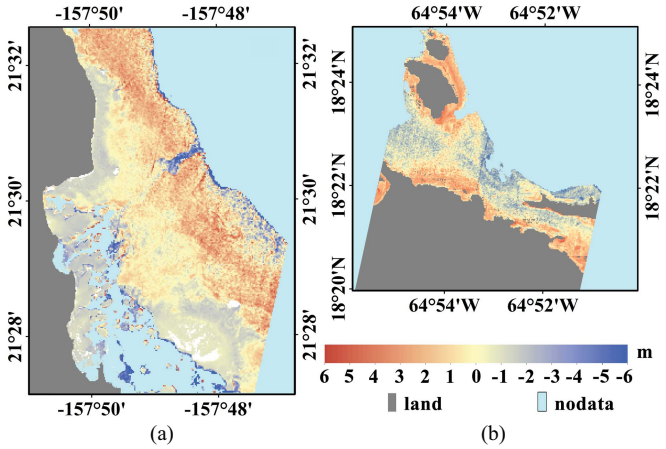

Fig. 9. Error distribution of estimated depths by the new method versus the LIDAR depths (estimated depth−LIDAR depth) (a) was calculated by subtracting LIDAR depth shown in Fig. 3(b) from the new model retrieved result shown in Fig. 5(b) and (b) was calculated by subtracting LIDAR depth shown in Fig. 3(c) from the new model retrieved result shown in Fig. 5(c).

LIDAR data were used to calibrate the coefficients of the linear transform method for every image. Figs. 7 and 8 show obvious noises, which were caused by the form of the linear transform method. The method is constituted by the ratio of only two bands. Additionally, the accuracy of the method is poor for depths between 0 and 5 m because the ratio of the green and blue bands is sensitive to the substrate type over the shallow water [14], [16]. From these results, we can also find that both our method and the linear transform method performed poorly over deep water (> 20 m). Compared with the Stumpf *et al.* method, our proposed method has the following advantages: 1) the coefficients in our model need to be calibrated only once for the same hyperspectral sensor and similar water areas, and 2) for very shallow water (< 5 m), the proposed method performs better than the Stumpf *et al*. method because it can reduce the influence of the substrate type; and 3) the proposed method can reduce the noise of the data rather than enhance it, as the Stumpf *et al*. method does.

V. Conclusion

The error distribution of the proposed method is shown in Fig. 9 to analyze the error source. In the figure, the absolute error of the method increases with depth, and the systematic bias appears over deep water (> 20 m). The light was hardly detected by the sensor after attenuation through deep water. In other words, the curve of the spectrum would vary slightly with the increased depth in deep water, which caused the systematic bias [4]. There are many outliers in some regions; the marginal region of the coral reef body and the region with exceptional data points appeared as stripes. Many factors may have led to these errors. The LIDAR data were preprocessed using a spatial averaging algorithm to ensure that its spatial resolution was the same as the Hyperion data. Additionally, the Hyperion data have an uncertainty of approximately 100 m in the horizontal positional accuracy. During the process of registering these data, many errors were generated. There are stripe noises in the Hyperion data, which led to radiance error of these pixels and the bathymetry errors. According to Lee *et al.* [35], 15% of the overall error for these processes could be bathymetry errors.

An algorithm based on the water's spectral characteristics was developed to retrieve the bathymetry of clear, shallow coastal water. Two parameters (SC and CC) were introduced in the model to describe the changes of spectrum caused by benthic and water reflectance, respectively. Although more studies are needed to verify the robustness of the model, three experimental results indicated that our proposed method had a fairly good and robust performance over shallow water (< 20 m). Compared with the similar linear transform method proposed by Stumpf *et al*., our proposed method can better overcome the influence of the substrate and the data noise. The two coefficients in the method also need to be calibrated by some field data, but they only need to be calibrated once for the same sensor and similar water area. Because the water optical properties were assumed to be uniform here, our method may perform well only over clean water with uniform water properties. Therefore, much more work will be performed to verify and improve the thoughts presented in this paper.

Acknowledgment

The SHOALS–LIDAR data were provided by the U.S. Geological Survey (http://www.soest.hawaii.edu/coasts/data/oahu/shoals.html). The Hyperion imageries were also provided by USGS (http://earthexplorer.usgs.gov/). The Fugro's Airborne LIDAR data were provided by NOAA (http://ccma.nos.noaa.gov/ecosystems/coralreef/usvi_nps.aspx).

References

[1] D. R. Lyzenga, N. R. Malinas, and F. J. Tanis, "Multispectral bathymetry using a simple physically based algorithm," *IEEE Trans. Geosci. Remote Sens.*, vol. 44, no. 8, pp. 2251–2259, Aug. 2006.

[2] C. L. Conger, E. J. Hochberg, C. H. Fletcher, and M. J. Atkinson, "Decorrelating remote sensing color bands from bathymetry in optically shallow waters," *IEEE Trans. Geosci. Remote Sens.*, vol. 44, no. 6, pp. 1655–1660, Jun. 2006.

[3] W. D. Philpot, "Bathymetric mapping with passive multispectral imagery," *Appl. Opt.*, vol. 28, no. 8, pp. 1569–1578, Apr. 1989.

[4] R. P. Stumpf, K. Holderied, and M. Sinclair, "Determination of water depth with high-resolution satellite imagery over variable bottom types," *Limnol. Oceanogr.*, vol. 48, no. 1, pp. 547–556, Jan. 2003.

[5] D. R. Lyzenga, "Passive remotesensing techniques for mapping water depth and bottom features," *Appl. Opt.*, vol. 17, no. 3, pp. 379–383, 1978.

[6] V. E. Brando, J. M. Anstee, M. Wettle, A. G. Dekker, S. R. Phinn, and C. Roelfsema, "A physics based retrieval and quality assessment of bathymetry from suboptimal hyperspectral data," *Remote Sens. Environ.*, vol. 113, no. 4, pp. 755–770, Apr. 2009.

[7] Z. Lee, K. L. Carder, R. F. Chen, and T. G. Peacock, "Properties of the water column and bottom derived from airborne visible infrared imaging spectrometer (AVIRIS) data," *J. Geophys. Res., Oceans*, vol. 106, no. C6, pp. 11639–11651, Jun. 2001.

[8] D. R. Lyzenga, "Remote sensing of bottom reflectance and water attenuation parameters in shallow water using using aircraft and Landsat data," *Int. J. Remote Sens.*, vol. 2, no. 1, pp. 71–82, 1981.

[9] R. K. Clark, T. H. Fay, and C. L. Walker, "Bathymetry calculations with Landsat 4 TM imagery under a generalized ratio assumption," *Appl. Opt.*, vol. 26, no. 19, pp. 4036–4038, Oct. 1987.

[10] V. Lafon, J. M. Froidefond, F. Lahet, and P. Castaing, "SPOT shallow water bathymetry of a moderately turbid tidal inlet based on field measurements," *Remote Sens. Environ.*, vol. 81, no. 1, pp. 136–148, Jul. 2002.

[11] S. Andrefouet, P. Kramer, D. Torres-Pulliza, K. E. Joyce, E. J. Hochberg, R. Garza-Perez, P. J. Mumby, B. Riegl, H. Yamano, W. H. White, M. Zubia, J. C. Brock, S. R. Phinn, A. Naseer, B. G. Hatcher, and F. E. Muller-Karger, "Multi-site evaluation of IKONOS data for classification of tropical coral reef environments," *Remote Sens. Environ.*, vol. 88, nos. 1–2, pp. 128–143, Nov. 2003.

[12] A. H. Benny and G. J. Dawson, "Satellite imagery as an aid to bathymetric charting of the Red Sea," *Cartogr. J.*, vol. 20, no. 1, pp. 5–16, 1983.

[13] D. R. Lyzenga, "Shallow-water bathymetry using combined lidar and passive multispectral scanner data," *Int. J. Remote Sens.*, vol. 6, no. 1, pp. 115–125, 1985.

[14] M. A. Camacho, "Depth analysis of Midway Atoll using QuickBird multi-spectral imaging over variable substrates," M.S. thesis, Dept. Space Syst. Oper., Naval Postgraduate School, Monterey, CA, USA, 2006.

[15] M. J. Loomis, "Depth derivation from the worldview-2 satellite using hyperspectral imagery," M.S. thesis, Dept. Meteorol., Naval Postgraduate School, Monterey, CA, USA, 2009.

[16] R. E. Clark, "Naval satellite bathymetry: A performance assessment," M.S. thesis, Dept. Meteorol., Naval Postgraduate School, Monterey, CA, USA, 2005.

[17] J. C. Sandidge, and R. J. Holyer, "Coastal bathymetry from hyperspectral observations of water radiance," *Remote Sens. Environ.*, vol. 65, no. 3, pp. 341–352, Sep. 1998.

[18] Z. P. Lee, K. L. Carder, C. D. Mobley, R. G. Steward, and J. S. Patch, "Hyperspectral remote sensing for shallow waters. I. A semianalytical model," *Appl. Opt.*, vol. 37, no. 27, pp. 6329–6338, Sep. 1998.

[19] Z. Lee, B. Casey, R. Arnone, A. Weidemann, R. Parsons, M. J. Montes, B.-C. Gao, W. Goode, C. Davis, and J. Dye, "Water and bottom properties of a coastal environment derived from Hyperion data measured from the EO-1 spacecraft platform," *J. Appl. Remote Sens.*, vol. 1, no. 1, p. 011502, 2007.

[20] Z. P. Lee, K. L. Carder, C. D. Mobley, R. G. Steward, and J. S. Patch, "Hyperspectral remote sensing for shallow waters: 2. Deriving bottom depths and water properties by optimization," *Appl. Opt.*, vol. 38, no. 18, pp. 3831–3843, Jun. 1999.

[21] S. M. Adler-Golden, P. K. Acharya, A. Berk, M. W. Matthew, and D. Gorodetzky, "Remote bathymetry of the littoral zone from AVIRIS, LASH, and QuickBird imagery," *IEEE Trans. Geoscis. Remote Sens.*, vol. 43, no. 2, pp. 337–347, Feb. 2005.

[22] J. A. Goodman and S. L. Ustin, "Classification of benthic composition in a coral reef environment using spectral unmixing," *J. Appl. Remote Sens.*, vol. 1, no. 1, p. 011501, 2007.

[23] M. L. McIntyre, D. F. Naar, K. L. Carder, B. T. Donahue, and D. J. Mallinson, "Coastal bathymetry from hyperspectral remote sensing data: Comparisons with high resolution multibeam bathymetry," *Marine Geophys. Res.*, vol. 27, no. 2, pp. 128-136, Jun, 2006.

[24] C. Giardino, M. Bartoli, G. Candiani, M. Bresciani, and L. Pellegrini, "Recent changes in macrophyte colonisation patterns: An imaging spectrometry-based evaluation of southern Lake Garda (northern Italy)," *J. Appl. Remote Sens.*, vol. 1, no. 1, p. 011509, 2007.

[25] W. M. Klonowski, P. R. C. S. Fearns, and M. J. Lynch, "Retrieving key benthic cover types and bathymetry from hyperspectral imagery," *J. Appl. Remote Sens.*, vol. 1, no. 1, p. 011505, 2007.

[26] C. D. Mobley, L. K. Sundman, C. O. Davis, J. H. Bowles, T. V. Downes, R. A. Leathers, M. J. Montes, W. Paul Bissett, D. D. R. Kohler, R. P. Reid, E. M. Louchard, and A. Gleason, "Interpretation of hyperspectral remotesensing imagery by spectrum matching and look-up tables," *Appl. Opt.*, vol. 44, no. 17, pp. 3576–3592, Jun. 2005.

[27] A. Lim, J. D. Hedley, E. LeDrew, P. J. Mumby, and C. Roelfsema, "The effects of ecologically determined spatial complexity on the classification accuracy of simulated coral reef images," *Remote Sens. Environ.*, vol. 113, no. 5, pp. 965–978, May 2009.

[28] H. Holden and E. LeDrew, "Measuring and modeling water column effects on hyperspectral reflectance in a coral reef environment," *Remote Sens. Environ.*, vol. 81, nos. 2–3, pp. 300–308, Aug. 2002.

[29] D. Lubin, W. Li, P. Dustan, C. H. Mazel, and K. Stamnes, "Spectral signatures of coral reefs: Features from space," *Remote Sens. Environ.*, vol. 75, no. 1, pp. 127–137, Jan. 2001.

[30] L. Clarisse, F. Prata, J. L. Lacour, D. Hurtmans, C. Clerbaux, and P. F. Coheur, "A correlation method for volcanic ash detection using hyperspectral infrared measurements," *Geophys. Res. Lett.*, vol. 37, no. 19, p. L19806, Oct. 2010.

[31] S. G. Ungar, J. S. Pearlman, J. A. Mendenhall, and D. Reuter, "Overview of the Earth Observing One (EO-1) mission," *IEEE Trans. Geosci. Remote Sens.*, vol. 41, no. 6, pp. 1149–1159, Jun. 2003.

[32] H. Q. Xu, "Modification of normalised difference water index (NDWI) to enhance open water features in remotely sensed imagery," *Int. J. Remote Sens.*, vol. 27, no. 14, pp. 3025–3033, Jul. 2006.

[33] Y. Xu, R. Wang, S. Liu, S. Yang, and B. Yan, "Atmospheric correction of hyperspectral data using MODTRAN model," *Proc. SPIE*, vol. 7123, p. 712306, Nov. 2008.

[34] T. Kutser, E. Vahtmae, and J. Praks, "A sun glint correction method for hyperspectral imagery containing areas with non-negligible water leaving NIR signal," *Remote Sens. Environ.*, vol. 113, no. 10, pp. 2267–2274, Oct. 2009.

[35] Z. P. Lee, B. Casey, R. Parsons, W. Goode, A. Weidemann, and R. Arnone, "Bathymetry of shallow coastal regions derived from space-borne hyperspectral sensor," in *Proc. MTS/IEEE OCEANS* 2005, pp. 2160–2170, Sep. 2005.

Sheng Ma received the B.S. degree in resources science and technology from the Beijing Normal University, Beijing, China, in 2005. He is currently pursuing the Ph.D. degree in cartography and geographic information system with the Institute of Remote Sensing Applications, Chinese Academy of Sciences, Beijing, China.

His current research interests include satellite oceanography, optical image processing, and marine ecological studies.

Zui Tao was born in China, in 1984. He received the B.S degree in cartography and geographic information system from Henan University, Kaifeng, China, in 2005, the M.S degree in cartography and geographic information system from Wuhan University, Wuhan, China, in 2008, and the Ph.D. degree in cartography and geographic information system from the Institute of Remote Sensing Applications (IRSA), Chinese Academy of Sciences (CSA), Beijing, China, in 2012.

He is currently a Research Associate at IRSA, CSA. His current research interests include ocean color remote sensing, optical image processing, and marine environmental monitoring.

Xiaofeng Yang (S'07–M'11) received the B.S. degree in environment science from Sichuan University, Chengdu, China, in 2005, and the Ph.D. degree in cartography and geographic information system from the Institute of Remote Sensing Applications (IRSA), Chinese Academy of Sciences (CAS), Beijing, China, in 2010.

He was a Visiting Research Scientist with the Department of Atmospheric and Oceanic Science, University of Maryland, College Park, MD, USA, from 2009 to 2010, during his Ph.D. program. He has been with the IRSA, CAS, since 2010. He has also participated in developing various types of operational ocean products in China coastal waters from environmental satellite data. His current research interests include satellite oceanography, marine and atmospheric pollution monitoring, synthetic aperture radar image processing, and marine atmospheric boundary layer process studies.

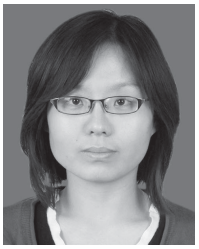

Yang Yu received the B.S degree in cartography and geographic information system from the Shanghai Institute of Technology, Shanghai, China, in 2005, the M.S degree in physical oceanography from the First Institute of Oceanography, State Oceanic Administration of China, Qingdao, China, in 2010. She is currently pursuing the Ph.D. degree in cartography and geographic information system with the Institute of Remote Sensing Applications (IRSA), Chinese Academy of Sciences (CSA), Beijing, China.

She is currently a Research Associate at IRSA, CSA. Her current research interests include marine dynamics, and marine environmental monitoring.

Xuan Zhou received the Ph.D. degree in cartography and geographic information system from the Institute of Remote Sensing Applications, Chinese Academy of Sciences, Beijing, China, in 2012.

His current research interests include satellite oceanography, typhoon observation, and radar remote sensing.

Ziwei Li received the B.S. and M.S. degrees in photogrammetry and remote sensing from the People's Liberation Army (PLA) Information Engineering University, Zhengzhou, China, in 1982 and 1990, respectively.

She was an Assistant Professor with the Department of Geomatics, PLA Information Engineering University, before joining the Chinese Academy of Surveying and Mapping, Beijing, China, in 1996. From 2006 to 2007, she was a Research Fellow with the First Institute of Oceanography, State Oceanic Administration of China, Qingdao, China. Since 2008, she has been with the Institute of Remote Sensing Applications, Chinese Academy of Sciences, Beijing, China. Her current research interests include the application of remote sensing data for oceanography and meteorology studies.